Reduced coupling of water molecules near the surface of reverse micelles

Bakulin, Artem A.; Pshenichnikov, Maxim S.

Published in:
Physical Chemistry Chemical Physics

DOI:
10.1039/c1cp22235j

Publication date:
2011

PCCP

Cite this: *Phys. Chem. Chem. Phys.*, 2011, **13**, 19355–19361

www.rsc.org/pccp

PAPER

Reduced coupling of water molecules near the surface of reverse micelles

Artem A. Bakulin† and Maxim S. Pshenichnikov*

Received 8th July 2011, Accepted 2nd September 2011
DOI: 10.1039/c1cp22235j

We report on vibrational dynamics of water near the surface of AOT reverse micelles studied by narrow-band excitation, mid-IR pump–probe spectroscopy. Evidence of OH-stretch frequency splitting into the symmetric and asymmetric modes is clearly observed for the interfacial H_2O molecules. The polarization memory of interfacial waters is preserved over an exceptionally extended >10 ps timescale which is a factor of 100 longer than in bulk water. These observations point towards negligibly small intermolecular vibrational coupling between the water molecules as well as strongly reduced water rotational mobility within the interfacial water layer.

Introduction

Hydration shells of biological membranes play an important role in a wide range of chemical and biochemical processes including surface-specific reactions,[1] protein secondary structure stabilization,[2,3] and proton and energy transfer.[4,5] According to the current paradigm, water works as a building block and a lubricant for the biomachinary of the cell, and as an energy and charge transfer agent.[6] During the last few decades, various studies indicated that a broad distribution of water sites exists inside the proteins[7] and lipid layers making water a constitutive part of membranes.[8,9] In all cases, properties and functions of water molecules differ considerably depending on the particular molecular environment. Strongly altered hydrogen-bond dynamics in the lipid hydration shells have been observed in the experiments addressing water translational mobility, reorientation, and hydrogen-bond strength.[10–15] Interestingly, such studies indicate coupling between the dynamics of water and biological objects which may imply a strong interaction between the solute and the hydration shell.[16,17]

It is well known that structure, dynamics and even macroscopic properties of water are determined by the strong intermolecular interactions between the hydrogen-bonded water molecules.[18] However, the question which still remains unanswered is whether water molecules at interfaces, such as in the hydration layer of the membrane, display a behavior similar to the bulk water.[19] For instance, recent NMR studies indicated quite moderate average dynamic perturbations—of a factor of 2 for 90% of the hydration layer at room temperature.[20] It was also pointed out, however, that there exists a small fraction of specific hydration sites, where water rotations are strongly retarded. In contrast, from the neutron scattering experiments it was concluded that the diffusion coefficient of hydration water decreases as much as by a factor of 100, as compared to bulk water.[21] Furthermore, the hydration layer thickness inferred from THz measurements was found to extend to as long as $\sim$1.8 nm beyond the interface which comprises many water layers.[22] The lively discussion on these issues can be found in ref. 23; we only note here that all aforementioned techniques implicitly average a number of system realizations due to lack of the adequate temporal resolution. Therefore, the time constants determination has necessarily to rely on modeling especially in the case of dynamically heterogeneous systems.

Another approach that has promoted intensive research[24,25] is time-resolved IR spectroscopy of the OH/OD stretching modes, intermolecular coupling of which can serve as a reporter for the extent of water–water interactions. For example, it was shown that intermolecular couplings make water molecules behave collectively, and in this way they dramatically accelerate redistribution of vibrational and thermal energy through the hydrogen-bonded water network,[26–28] play essential role in the water mediated proton transfer[29–31] and other biologically relevant processes.[6] Nonetheless, in spite of a considerable effort in studying the dynamics and intermolecular coupling of water molecules bound to the different interfaces, the overall picture still remains controversial. For instance, sum-frequency generation (SFG) studies on water–silica[32] and water–air[33] interfaces have shown, quite surprisingly, that despite noticeable differences in spectral responses, the OH stretch vibrational dynamics of the surface water molecules are hardly distinguishable from those in the bulk. This suggests that water molecules at the surface are coupled either among themselves or to the water in the bulk phase. In contrast, SFG studies on charged surfaces,[34,35] water–lipid interfaces, and on hydrated membranes exposed noticeable changes in their vibrational dynamics compared to bulk water.[36] The interpretation of the results observed in various SFG studies is complicated by the fact that spatial selectivity of SFG (*i.e.* the extent of probed distances from the interface) at charged interfaces is still under debate.[37]

Department of Physical Chemistry, Zernike Institute for Advanced Materials, University of Groningen, Nijenborgh 4, 9747 AG Groningen, The Netherlands. E-mail: m.s.pchenitchnikov@rug.nl
† Current address: Cavendish Laboratory, University of Cambridge, J J Thomson Avenue, Cambridge CB3 0HE, UK.

On the other hand, ultrafast vibrational spectroscopy studies also evidenced a substantial deceleration of population relaxation rates[38] and a decrease in the induced anisotropy decay[39–42] of water vibrations in the lipid hydration layer. This implies completely different hydrogen-bond dynamics and effect of intermolecular couplings at the water–lipid interface. Quite surprisingly, the behavior observed in these experiments for isotopically pure water appears to be similar to the one in water isotopic mixtures, where inter- and intramolecular couplings are artificially broken by isotopic dilution.[43,44] Nonetheless, experiments which are capable of a more direct elucidation of the inter- and intramolecular dynamics[45] in the membrane hydration layer (for example, by selectively addressing dynamics at different vibrational frequencies) have not been reported yet.

Reverse micelles, which are nanodroplets of water covered with a monolayer of lipid-like surfactant and floating in a nonpolar solvent, present a convenient model system to mimic the membrane interfaces. The previous studies[38,39,46–51] indicated the existence of a layered structure of the nano-droplet interior, consisting of bulk-like water in the micelle "core" and a fraction of "shell" water near the interface. This partitioning of water molecules into two sub-ensembles makes the reverse micelle an excellent model for interfacial water (in small, $d = 1$ nm micelles the fraction of border-effected water is more than 80%) and almost bulk-like water (in large $d = 10$ nm diameter micelles the fraction of core water approaches 90%). The separation of water into two sub-ensembles is also supported by the results of previous IR nonlinear experiments on the reverse micelles;[38,39,43,44,52–54] however, some deviations from the core–shell model have also been reported.[55,56]

Earlier studies of water vibrational dynamics in AOT reverse micelles[38,39] were focused on verifying the core–shell model in the case of H_2O molecules where OH stretches are strongly coupled. In particular, it was demonstrated that the bulk-water core of the micelle is decoupled from the water at the micelle interface. However, not much insight was provided into the properties of the aqueous environment of the micelle hydration shell because of limitations imposed by the broadband excitation. In such experiments, the broadband excitation is not spectrally-selective thereby leading to the population of the whole range of intra- and intermolecular modes. This considerably complicates the disentanglement of different contributions to the spectroscopic observables, and does not allow for a direct interpretation of the experimental results. One way to avoid the aforementioned problem in exploring the dynamics at the frequencies of different spectral signatures is to use selective excitation, either by using coherent multidimensional spectroscopy[57–62] or by narrowing the bandwidth of the excitation pulses.[43]

In this paper, we investigate the extent of the intermolecular vibrational coupling between the OH stretching modes of water molecules in the lipid hydration shell. The vibrational anisotropy dynamics are selectively induced by a (relatively) narrow-band IR excitation of the OH stretching modes of water in small (diameter of 1 nm) reverse micelles where most water molecules are interface-bound, and compare its behaviour with that observed in the large (diameter of 10 nm) ones. We clearly observe evidence of splitting of OH-stretch vibrations of the H_2O molecule near the lipid interface of AOT reverse micelles into the symmetric and asymmetric modes. Furthermore, the transition dipole orientation of such vibrations appears to be preserved at an exceptionally long 10-ps timescale—a factor of 100 longer than in the bulk phase. The strongly reduced anisotropy decay signifies negligibly small intermolecular interactions among water molecules in the interfacial water layer as well as their weak coupling to the bulk-like core water.

Following our previous approach, we, unlike others who mostly studied isotopically diluted water, focus on the H_2O-filled micelles. At a first glance, this strategy is not likely to yield any information on rotational mobility of water molecules as the anisotropy dynamics (*i.e.* the memory for the direction of the initially-excited transient dipole) in neat water are known to be governed by *inter*molecular energy transfer due to substantial coupling between OH oscillators on different molecules.[24,63] As a consequence, the anisotropy is scrambled within $\sim$100 fs which is one order of magnitude faster than the actual timescale of water rotational diffusion of $\sim$1.5 ps.[64–66] However, this argument can be reverted as follows: if the water anisotropy does not decay that quick, the intermolecular coupling should be considerably decreased which allows deriving information on, for instance, the intermolecular separations as was demonstrated by Bakker and co-workers[26,67] for water isotopically diluted at different concentrations.

Experimental

Reverse micelles were prepared by mixing and stirring for 10 min bis(2-ethylhexyl) sulfosuccinate (AOT) from Aldrich and octane (Janssen Chimica) at a concentration of $\sim$100 g l^{-1}. Then water (Aldrich, HPLC grade) was added to the solution. The reverse micelles are conventionally characterized[51] either by the ratio of water to surfactant $w_0 = [H_2O]/[AOT]$ or the water core diameter which for the AOT micelles is directly proportional to w_0;[68] the last parameter will be used throughout the current paper. For reverse micelles with isotopically diluted water, 5% solution of HDO in D_2O was used instead of H_2O. In this case, the minimal possible diameter of HDO/D_2O micelles was $\sim$1.6 nm, which was dictated by the residual AOT hydration. All preparation was performed under ambient conditions. The resulted solution was further diluted with octane until the water concentration was about 0.3 mol l^{-1}, which gives a maximum optical density of $\sim$0.4 (the sample thickness of $\sim$50 μm) at the measurement wavelength of $\sim$3 μm.

For the polarization sensitive pump–probe experiments, infrared (IR) pulses were produced by an optical parametrical generator[69] pumped by a 1 kHz Ti:Sapphire multipass amplifier. The mid-IR pulses were tunable around 3500 cm^{-1} and had a duration of about 70 fs with a bandwidth of 320 cm^{-1} FWHM. The generated pulses were split in a 3 μJ pump pulse and a $<$0.1 μJ probe pulse. Then, after passing through the delay stages, both pulses were focused into the $\sim$50 μm thick free-falling jet sample.[70]

The polarization of the probe beam was rotated by 45° with respect to the polarization of the pump beam. After the sample, the probe component parallel or perpendicular to the pump polarization was selected by a wire-grid polarizer (1 : 100 extinction), spectrally dispersed in a polychromator and recorded by a liquid-nitrogen-cooled 64-element MCT array.

The photo-induced anisotropy $r(t)$ (that is a measure for polarization memory) was calculated as[71]

$$r(t) = \frac{\Delta T_{\parallel}(t) - \Delta T_{\perp}(t)}{\Delta T_{\parallel}(t) + 2\Delta T_{\perp}(t)}, \qquad (1)$$

where $\Delta T_{\parallel}$ and $\Delta T_{\perp}$ are the relative transmission changes for the parallel and perpendicular components of the probe, respectively. All experiments were performed at ambient conditions.

To achieve selective excitation of the OH-stretch modes, pump pulses with a narrowed spectrum were generated in the following way: cut-off spectral filters were made of either a HDO : D_2O filled, 50 μm thick CaF_2 cell (to achieve excitation at 3590 cm^{-1}) or of the same cell filled with 1% solution of H_2O in acetonitrile (to achieve excitation at 3450 cm^{-1}). The respective solutions absorbed all radiation with frequencies below or above 3500 cm^{-1}, thereby allowing relatively narrow bandwidth (~100 cm^{-1}) excitation in the region of interest. Resulted temporal resolution, calculated from the signal rise-time, was better than 150 fs. To ensure a better spectral selectivity, experiments were also performed with a narrow-band Fabry–Pérot interferometer inserted in the pump beam,[72,73] which provided a higher spectrum selectivity (down to ~40 cm^{-1}) at the expense of a decreased signal-to-noise ratio and time resolution. These experiments yielded similar results to those observed with the wider excitation spectra.

Results and discussion

Fig. 1 compares absorption spectra of OH stretching modes of H_2O confined in 1 nm and 10 nm diameter reverse micelles (w_0 = 1 and w_0 = 35, respectively) and HDO confined in 1.6 nm micelles (w_0 = 2). The absorption spectrum for d = 10 nm micelles, which contain a few thousands of water molecules,[51] follows closely the absorption spectrum of bulk water (not shown), some blue shift notwithstanding. This is corroborated by the fact that ~90% of water molecules in d = 10 nm reverse micelles find themselves in the "bulk-like" environment of the core.[39,44,48] In contrast, absorption of the OH stretching mode for the small reverse micelles, containing ~30 waters,[43,51] displays a pronounced blue shift and spectral narrowing. The blue shift of the OH vibrational frequency is usually attributed to weaker (on average) hydrogen bonds between the water molecules.[74,75] In the d = 1 nm reverse micelles 90% of water molecules border the lipid wall, hence the observed blue shift of the OH stretch indicates a strongly weakened hydrogen-bond environment near the water–AOT interface.

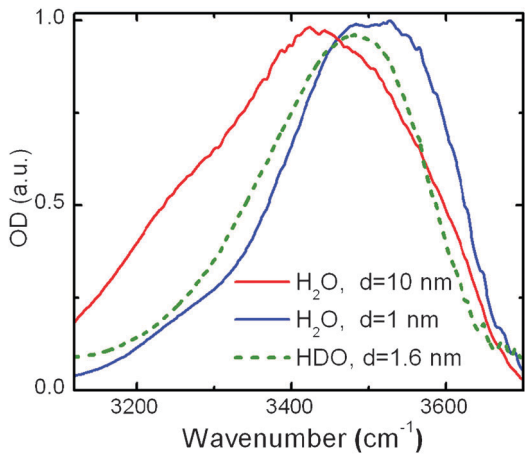

Fig. 1 Absorption spectra of 10 nm (red curve) and 1 nm (blue curve) diameter reverse micelles in the OH stretching mode region. Solid curves show absorption of the H_2O-filled reverse micelles while the dashed green curve represents the absorption spectrum of 1.6 nm diameter micelles filled with a 5% solution of HDO in D_2O.

The OH-stretch absorption profile of H_2O in d = 1 nm reverse micelles has a complex shape where at least three different resonances at ~3280, 3450, and 3580 cm^{-1} can be recognized. There are three effects contributing to the absorption spectrum shape: inhomogeneous distribution of water sites, intramolecular coupling between the two OH oscillators of a water molecule, and dipole–dipole intermolecular coupling between OH-oscillators of different water molecules. The red shoulder of the 1 nm H_2O-filled reverse micelles (Fig. 1, blue curve) is most probably caused by the intermolecular coupling[63] among the core molecules because, first, it matches the red flank of bulk water absorption and, second, its amplitude strongly decreases upon water dilution (Fig. 1, dashed green curve). We attribute the resonances at 3590 cm^{-1} and 3450 cm^{-1} to intramolecular coupling between the two OH-stretch vibrations of the same water molecule because they merge into a single resonance at ~3500 cm^{-1} for HDO molecules, for which the stretching modes are no longer coupled due to the difference in their frequencies.

Recent linear[76] and non-linear[73,77] IR spectroscopy studies performed on reverse micelles and weakly hydrated phospholipid membranes indicated that there are at least three sub-ensembles of water molecules in the lipid hydration layer. Those sub-ensembles are: double hydrogen-bonded waters to other H_2O molecules, single hydrogen bonded waters, and non-hydrogen bonded waters with both hydrogen atoms adjacent to the membrane. Because of the difference in environment wherein the waters reside, the effects on inter- and intra-molecular couplings strongly depend on the particular configuration that the water molecules acquire. Therefore, mapping out the coupling strength in linear and nonlinear absorption spectra potentially allows elucidating information about the water site distributions and even about the particular way the water molecule interacts with the membrane or other water molecules. In this respect, measurements of spectrally-selective nonlinear responses are particularly useful because they selectively address a particular sub-ensemble of H_2O molecules[78] and provide information on dynamical structural exchange between the different hydrating configurations.[40]

Fig. 2 shows transient spectra obtained for d = 1 nm reverse micelles with a narrow bandwidth excitation at 50 fs delay for parallel and perpendicular polarizations of the pump and probe. The negative parts of the spectra correspond to ground-state bleaching of and/or excited-state emission of the OH-stretch transition while the positive parts are due to excited-state absorption. For 3590 cm^{-1} excitation and parallel pump–probe geometry, the ground-state-bleach signal follows reasonably well the excitation spectrum (Fig. 2a, red curve) which indicates a substantial inhomogeneous broadening of the absorption line. However, the response in perpendicular polarizations is much wider and has an additional peak at 3450 cm^{-1}.

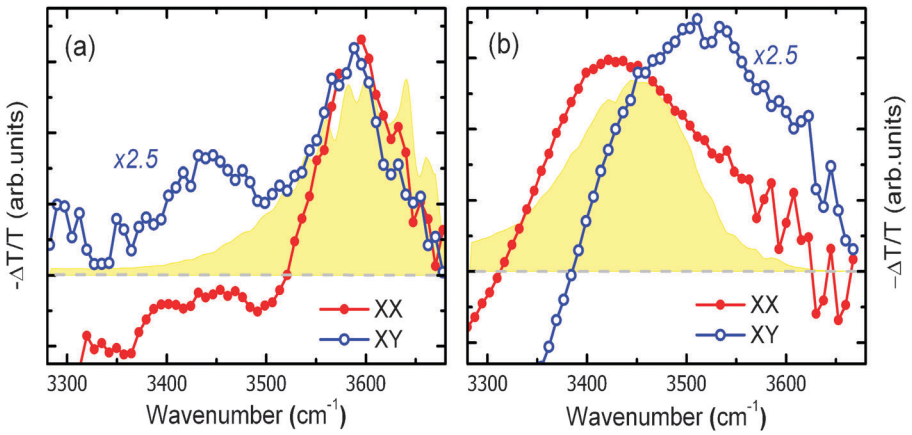

Fig. 2 Transient absorption spectra obtained in parallel (filled red circles) and perpendicular (open blue circles) polarization geometries for 1 nm size water-filled reverse micelles at a delay of 50 fs. The spectra were recorded with narrow-bandwidth excitation pulses centered at 3590 cm^{-1} (a) and 3450 cm^{-1} (b) with their respective photoexcitation spectra shown in yellow shades. The above-zero parts of the transient spectra correspond to the bleaching of the ground vibrational state and/or stimulated emission from the first excited state.

Therefore, there is an efficient coupling between the initially excited transition at 3590 cm^{-1} and the one at 3450 cm^{-1}. The fact that the bleaching of the 3450 cm^{-1} transition occurs already at 50 fs indicates that the two transitions share the same ground state.[45]

The early-time transient spectra with the 3450 cm^{-1} excitation (Fig. 2b) follow a similar trend: the excitation-like response at 3450 cm^{-1} substantial broadening toward the wavelength of 3600 cm^{-1} in the orthogonal one. However, the pattern is less pronounced due to interference with the excited-state transitions (the positive part of the signals).[45]

To establish the mutual orientation of the transition dipole moments of the two coupled transitions presumably situated at 3450 cm^{-1} and 3590 cm^{-1} and sharing the same ground state, we calculated the spectrally-resolved transient anisotropy according to eqn (1) at different delays (Fig. 3). In the excitation region of 3590 cm^{-1} anisotropy decays slightly from the initial value of 0.4 to ~0.3 at 1 ps delay (Fig. 3a). A similar trend is observed in the vicinity of the 3450 cm^{-1} excitation where the anisotropy decays from 0.37 to ~0.1 during the first 1 ps (Fig. 3b). However, at the probe wavelength of 3590 cm^{-1}, anisotropy *increases* from the negative value of about −0.05 within 250 fs to decay at later times (Fig. 3b). In the complimentary experiment, with excitation at 3590 cm^{-1} and probe at 3450 cm^{-1}, the anisotropy also increases from negative values. However, the anisotropy behavior is more complex due to interference of the excited-state transition of the 3450 cm^{-1} mode.[45,79]

The initial negative anisotropies at the frequencies of other transitions cannot be explained in a single-transition framework but is fully consistent with the model of two communicating orthogonal modes as it is the case for the symmetric and asymmetric modes of the H_2O molecule (note that although this designation is not entirely accurate because the modes are not fully delocalized[79] we will use it anyway for briefness). The observed anisotropy data are in line with those previously reported for diluted H_2O solutions where intermolecular coupling between OH oscillators of different water molecules was inhibited by either nonpolar[80] or moderately polar[45,79] solvents. Cringus *et al.* explained the prominent spectral dependence of the anisotropy in the frame of splitting of OH-oscillator vibrations into symmetric and asymmetric modes.[45,79] Similar effects were also reported in the IR studies of weakly hydrated membranes.[73] It was proposed that the presence of ultrafast exchange between different modes

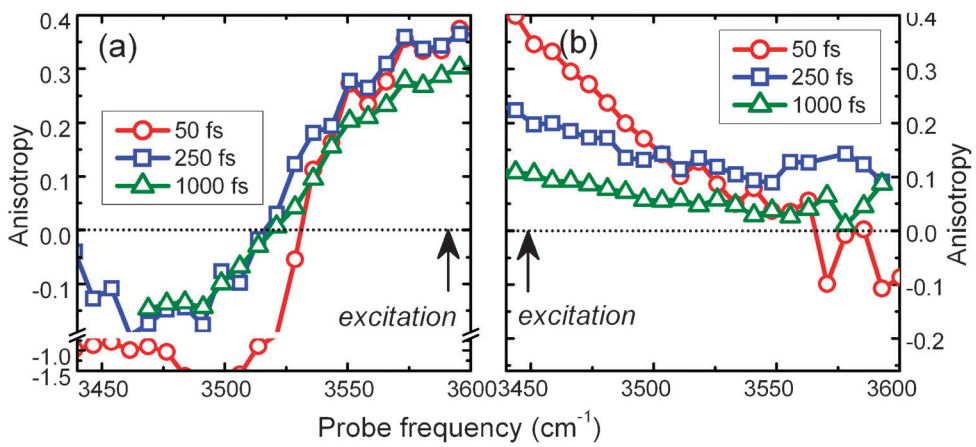

Fig. 3 Spectrally-resolved anisotropy obtained for 1 nm size, water-filled reverse micelles with narrow-bandwidth excitation pulses centered at 3590 cm^{-1} (a) and 3450 cm^{-1} (b). The delay times are: 50 fs (red circles), 250 fs (blue squares), and 1 ps (green triangles).

provides evidence for both OH oscillators being in a similar hydrogen-bonded configuration—both either bonded or non-bonded to neighboring water molecules.

The structure in steady-state (Fig. 1) and time-resolved (Fig. 2 and 3) vibrational spectra of the small reverse micelles can be associated with symmetric and asymmetric OH-stretch modes of water molecules. Judging from the substantial blue shift of the absorption spectra in small micelles, we can tentatively attribute the observed modes mostly to those water molecules which are adjacent to the reverse micelle membrane. These molecules are also decoupled from the surrounding water molecules because otherwise the OH vibrations would acquire a delocalized "excitonic" character due to strong intermolecular coupling[24,63] resulting in ultrafast anisotropy scrambling (*vide infra*). Therefore, the observed spectral and anisotropy dynamics indicate that water molecules in small reverse micelles are decoupled from one another, and most probably dominantly interact with the micelle wall.[39]

To verify that the communication between water molecules is suppressed near the micelle interface, we measured the anisotropy dynamics in small and large reverse micelles following narrow bandwidth excitation (Fig. 4). In all cases the anisotropy in small reverse micelles decays much slower than in the large ones where water properties are closer to those of bulk. As in the bulk water the anisotropy decay is dominated by intermolecular interactions between densely packed OH oscillators,[24,26,63,67] we conclude that these interactions are substantially weakened in small reverse micelles as is evident from the 3590 cm^{-1} excitation/probe data (Fig. 4a). In 1 nm size reverse micelles, after the initial 300 fs decay, the anisotropy levels off at a relatively high level of $\sim$0.25 and then slowly decays at the time scale of $\sim$20 ps (Fig. 4a, blue circles). Note that the accuracy of the latter value is rather limited because the pump–probe signal decreases with a vibrational population lifetime of $\sim$1 ps.[39,74] The timescale of 20 ps is in striking contrast with the ultrafast ($\sim$300 fs) anisotropy decay in the large size reverse micelles (Fig. 4a, red diamonds). Hence, suppression of the anisotropy decay in small reverse micelles can be ascribed to decoupling of OH oscillators of different water molecules and, therefore, inhibiting communication between different water molecules. The initial 30% decrease of anisotropy at 300 fs time scale originates from the population exchange due to intramolecular coupling between the symmetric and asymmetric stretches belonging to the same water molecule,[45] although some contribution from librations cannot be completely ruled out.[43,44] The subsequent slow decay of the anisotropy with a 20 ps time constant points towards extremely slow rotational diffusion of water molecules and general immobility of interfacial water. Similar long-lived polarization memory was also observed for water molecules trapped in a weakly hydrated membrane.[40]

At the 3430 cm^{-1} excitation/probe wavelength (Fig. 4b), the induced anisotropy in small reverse micelles also decays much slower than in the large ones (600 fs *vs.* 150 fs, respectively, with the later value being temporal resolution limited). The reason why in small reverse micelles the anisotropy at 3430 cm^{-1} does not slow down as much as at the excitation/probe wavelength of 3590 cm^{-1} is three-fold. First, at 3430 cm^{-1} there is a contribution from a quickly-decaying bulk-like core that even in small reverse micelles accounts for $\sim$20% of the water molecules (see, for instance, absorption spectra in Fig. 1). Second, the fundamental transition frequency of the symmetric mode at 3430 cm^{-1} is close to the frequency of the excited-state absorption of the asymmetric mode.[45] As the directions of the dipole moments of these transitions are close to orthogonal, their contributions interfere destructively in the anisotropy measurements thereby bringing the anisotropy value to zero. Finally, the long-term ps dynamics become hidden under the in-growing contribution of the essentially isotropic temperature response due to population relaxation of the core water[39] which maximum coincidently has a frequency of $\sim$3430 cm^{-1}. In this respect, the probe wavelength of 3590 cm^{-1} presents a window of opportunity as it is free of all aforementioned complications allowing the anisotropy dynamics to be followed at a 10 ps time scale.

The observation of slow rotational diffusion is well in line with the previous studies of isotopically diluted water in reverse micelles and phospholipid membranes.[40,41,81,82] Isotopic dilution leads to cancelation of both inter- and intramolecular couplings between OH (or OD) oscillators. In this case, transient

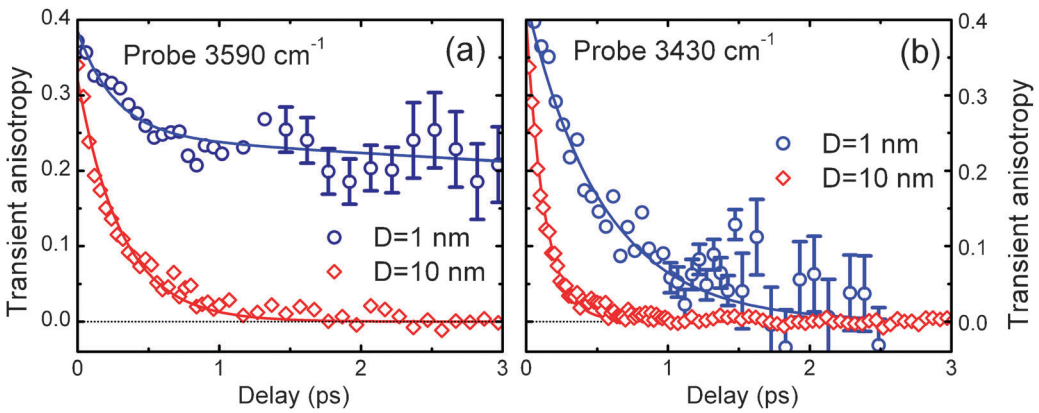

Fig. 4 Anisotropy dynamics following a narrow bandwidth excitation at 3590 cm^{-1} (a) and 3430 cm^{-1} (b) at the wavelengths of asymmetric and symmetric modes for d = 1 nm (blue circles) and 10 nm (red diamonds) reverse micelles. Solid curves present (bi)exponential fits to the experimental data points with time constants of 300 fs and 20 ps (panel a, blue curve), 300 fs (panel a, red curve), 600 fs (panel b, blue curve), 150 fs (panel b, red curve).

anisotropy experiments on an OH/OD oscillator would provide information explicitly on the orientational dynamics of water molecules. Furthermore, it was shown that at the micelle interface isotopically diluted water also displays extremely slow anisotropy decay, evidencing strongly compromised water reorientation and slow changes in the hydration layer environment.[40,81] The similarity between the current observations for H_2O confined in the reverse micelles, and the earlier ones on isotopically diluted water[43] indicates that intermolecular vibrational coupling is suppressed in both systems to a comparable extent. However, while the isotopic dilution inhibits intermolecular communication only by increasing the distance between the OH oscillators,[83] the presence of the micelle wall may also act in a different way. For instance, reduction of the intramolecular vibrational coupling can originate from a wide (quasi)static distribution of OH frequencies, caused by extremely slow dynamics in the hydration layer environment. This hypothesis can be potentially verified in a 2D IR experiment[61] on the H_2O filled reverse micelles which will be reported elsewhere.

Conclusions

In this paper, the effect of the lipid-like surface on the properties of the interfacial layer of water molecules has been studied by time-resolved narrowband pump—broadband probe spectroscopy. We have primarily focused on the dynamics of pure H_2O molecules rather than on the more conventional systems of HDO molecules diluted in either H_2O or D_2O. The reason for this is that bulk water spectroscopy has revealed a number of peculiar features (*e.g.*, ultrafast anisotropy decay) that arise from strong intermolecular couplings between the OH oscillators. Therefore, the pronouncement of these features can be a measure for the strength of the intermolecular coupling between the water molecules. As a reference, large reverse micelles with the water properties close to the bulk have also been studied.

Our results demonstrate that the hydrogen bond environment near the surface is completely different from the bulk water. First, the rotational mobility of water in the interfacial layer is suppressed by at least one order of magnitude as compared to bulk water. Second, the intermolecular energy transport that is characteristic for bulk water is so strongly inhibited within the interfacial water layer that there is little difference between vibrational dynamics of H_2O and naturally-decoupled, isolated HDO molecules. Finally, the observed splitting of OH-stretch absorption band into symmetric and asymmetric modes (both strongly inhomogeneously broadened) is another sign of weak interaction between the water molecules within the interfacial layer. All these features supposedly originate from the suppressed interactions between water molecules and from a dominant bonding of water molecules to the lipid membrane. The presented results are relevant for understanding the interactions of biological lipid membranes with the surrounding aqueous bath.

Acknowledgements

We thank Douwe Wiersma, Mischa Bonn, Hiub Bakker, Eric Borguet, Jim Skinner, and Thomas la Cour Jansen for many useful discussions, Dan Cringus for help with experimental setup, and Ben Hesp for critically reading the manuscript. A.A.B. acknowledges support from Netherlands Organisation for Scientific Research (NWO) through the Rubicon grant.

References

1 I. Benjamin, *Acc. Chem. Res.*, 1995, **28**, 233–239.
2 R. U. Lemieux, *Acc. Chem. Res.*, 1996, **29**, 373–380.
3 M. Chaplin, *Nat. Rev. Mol. Cell Biol.*, 2006, **7**, 861–866.
4 N. Agmon, *Chem. Phys. Lett.*, 1995, **244**, 456–462.
5 A. Remorino, I. V. Korendovych, Y. Wu, W. F. DeGrado and R. M. Hochstrasser, *Science*, 2011, **332**, 1206–1209.
6 P. Ball, *Chem. Rev.*, 2008, **108**, 74–108.
7 A. Ghosh, J. Qiu, W. F. DeGrado and R. M. Hochstrasser, *Proc. Natl. Acad. Sci. U. S. A.*, 2011, **108**, 6115–6120.
8 K. Takano, Y. Yamagata and K. Yutani, *Protein Eng.*, 2003, **16**, 5–9.
9 J. Milhaud, *Biochim. Biophys. Acta, Biomembr.*, 2004, **1663**, 19–51.
10 V. Kurze, B. Steinbauer, T. Huber and K. Beyer, *Biophys. J.*, 2000, **78**, 2441–2451.
11 Z. Zhou, B. G. Sayer, D. W. Hughes, R. E. Stark and R. M. Epand, *Biophys. J.*, 1999, **76**, 387–399.
12 K. Gawrisch, H. C. Gaede, M. Mihailescu and S. H. White, *Eur. Biophys. J.*, 2007, **36**, 281–291.
13 F. Foglia, M. J. Lawrence, C. D. Lorenz and S. E. McLain, *J. Chem. Phys.*, 2010, **133**, 145103.
14 D. Zhong, S. K. Pal and A. H. Zewail, *Chem. Phys. Lett.*, 2010, **503**, 1–11.
15 M. Tehei, B. Franzetti, K. Wood, F. Gabel, E. Fabiani, M. Jasnin, M. Zamponi, D. Oesterhelt, G. Zaccai, M. Ginzburg and B. Z. Ginzburg, *Proc. Natl. Acad. Sci. U. S. A.*, 2007, **104**, 766–771.
16 D. J. Tobias, N. Sengupta and M. Tarek, *Faraday Discuss.*, 2009, **141**, 99–116.
17 K. Wood, M. Plazanet, F. Gabel, B. Kessler, D. Oesterhelt, D. J. Tobias, G. Zaccai and M. Weik, *Proc. Natl. Acad. Sci.*, 2007, **104**, 18049–18054.
18 F. Franks, *Water: a comprehensive treatise*, Plenum Press, New York, 1972.
19 G. Stirnemann, P. J. Rossky, J. T. Hynes and D. Laage, *Faraday Discuss.*, 2010, **146**, 263–281.
20 J. Qvist, E. Persson, C. Mattea and B. Halle, *Faraday Discuss.*, 2009, **141**, 131–144.
21 A. Frolich, F. Gabel, M. Jasnin, U. Lehnert, D. Oesterhelt, A. M. Stadler, M. Tehei, M. Weik, K. Wood and G. Zaccai, *Faraday Discuss.*, 2009, **141**, 117–130.
22 B. Born, S. J. Kim, S. Ebbinghaus, M. Gruebele and M. Havenith, *Faraday Discuss.*, 2009, **141**, 161–173.
23 General Discussion, *Faraday Discuss.*, 2009, **141**, 81–98.
24 D. Kraemer, M. L. Cowan, A. Paarmann, N. Huse, E. T. J. Nibbering, T. Elsaesser and R. J. D. Miller, *Proc. Natl. Acad. Sci. U. S. A.*, 2008, **105**, 437–442.
25 A. Paarmann, T. Hayashi, S. Mukamel and R. J. D. Miller, *J. Chem. Phys.*, 2008, **128**, 191103.
26 S. Woutersen and H. J. Bakker, *Nature*, 1999, **402**, 507–509.
27 J. Lindner, P. Vohringer, M. S. Pshenichnikov, D. Cringus, D. A. Wiersma and M. Mostovoy, *Chem. Phys. Lett.*, 2006, **421**, 329–333.
28 S. Ashihara, N. Huse, A. Espagne, E. T. J. Nibbering and T. Elsaesser, *J. Phys. Chem. A*, 2007, **111**, 743–746.
29 S. Woutersen and H. J. Bakker, *Phys. Rev. Lett.*, 2006, **96**, 138305.
30 M. Bonn, H. J. Bakker, G. Rago, F. Pouzy, J. R. Siekierzycka, A. M. Brouwer and D. Bonn, *J. Am. Chem. Soc.*, 2009, **131**, 17070.
31 O. F. Mohammed, D. Pines, J. Dreyer, E. Pines and E. T. J. Nibbering, *Science*, 2005, **310**, 83–86.
32 J. A. McGuire and Y. R. Shen, *Science*, 2006, **313**, 1945–1948.
33 M. Smits, A. Ghosh, M. Sterrer, M. Muller and M. Bonn, *Phys. Rev. Lett.*, 2007, **98**, 098302.
34 A. Eftekhari-Bafrooei and E. Borguet, *J. Am. Chem. Soc.*, 2009, **131**, 12034–12035.
35 A. Eftekhari-Bafrooei and E. Borguet, *J. Am. Chem. Soc.*, 2010, **132**, 3756–3761.
36 A. Ghosh, M. Smits, J. Bredenbeck and M. Bonn, *J. Am. Chem. Soc.*, 2007, **129**, 9608–9609.
37 A. Eftekhari-Bafrooei and E. Borguet, *J. Phys. Chem. Lett.*, 2011, **2**, 1353–1358.

38 D. Cringus, J. Lindner, M. T. W. Milder, M. S. Pshenichnikov, P. Vohringer and D. A. Wiersma, *Chem. Phys. Lett.*, 2005, **408**, 162–168.
39 D. Cringus, A. Bakulin, J. Lindner, M. S. Pshenichnikov, P. Vohringer and D. A. Wiersma, *J. Phys. Chem. B*, 2007, **111**, 14193–14207.
40 V. V. Volkov, D. J. Palmer and R. Righini, *J. Phys. Chem. B*, 2007, **111**, 1377–1383.
41 D. E. Moilanen, E. E. Fenn, D. Wong and M. D. Fayer, *J. Phys. Chem. B*, 2009, **113**, 8560–8568.
42 D. E. Moilanen, E. E. Fenn, D. Wong and M. D. Fayer, *J. Am. Chem. Soc.*, 2009, **131**, 8318–8328.
43 A. M. Dokter, S. Woutersen and H. J. Bakker, *Proc. Natl. Acad. Sci. U. S. A.*, 2006, **103**, 15355–15358.
44 I. R. Piletic, D. E. Moilanen, D. B. Spry, N. E. Levinger and M. D. Fayer, *J. Phys. Chem. A*, 2006, **110**, 4985–4999.
45 D. Cringus, T. L. C. Jansen, M. S. Pshenichnikov and D. A. Wiersma, *J. Chem. Phys.*, 2007, **127**, 084507.
46 A. Maitra, *J. Phys. Chem.*, 1984, **88**, 5122–5125.
47 B. Baruah, J. M. Roden, M. Sedgwick, N. M. Correa, D. C. Crans and N. E. Levinger, *J. Am. Chem. Soc.*, 2006, **128**, 12758–12765.
48 N. E. Levinger, *Science*, 2002, **298**, 1722–1723.
49 H. S. Tan, I. R. Piletic, R. E. Riter, N. E. Levinger and M. D. Fayer, *Phys. Rev. Lett.*, 2005, **94**, 057405.
50 H.-S. Tan, I. R. Piletic and M. D. Fayer, *J. Chem. Phys.*, 2005, **122**, 174501.
51 N. E. Levinger and L. A. Swafford, *Annu. Rev. Phys. Chem.*, 2009, **60**, 385–406.
52 T. Patzlaff, M. Janich, G. Seifert and H. Graener, *Chem. Phys.*, 2000, **261**, 381–389.
53 H. S. Tan, I. R. Piletic and M. D. Fayer, *J. Chem. Phys.*, 2005, **122**, 174501.
54 J. C. Deak, Y. Pang, T. D. Sechler, Z. Wang and D. D. Dlott, *Science*, 2004, **306**, 473–476.
55 J. Chowdhary and B. M. Ladanyi, *J. Phys. Chem. B*, 2009, **113**, 15029–15039.
56 D. E. Moilanen, E. E. Fenn, D. Wong and M. D. Fayer, *J. Chem. Phys.*, 2009, **131**, 014704.
57 J. B. Asbury, T. Steinel, C. Stromberg, K. J. Gaffney, I. R. Piletic, A. Goun and M. D. Fayer, *Phys. Rev. Lett.*, 2003, **91**, 237402.
58 J. J. Loparo, S. T. Roberts and A. Tokmakoff, *J. Chem. Phys.*, 2006, **125**, 194521.
59 A. A. Bakulin, C. Liang, T. la Cour Jansen, D. A. Wiersma, H. J. Bakker and M. S. Pshenichnikov, *Acc. Chem. Res.*, 2009, **42**, 1229–1238.
60 A. A. Bakulin, M. S. Pshenichnikov, H. J. Bakker and C. Petersen, *J. Phys. Chem. A*, 2011, **115**, 1821–1829.
61 E. E. Fenn, D. B. Wong and M. D. Fayer, *J. Chem. Phys.*, 2011, **134**, 054512.
62 S. Garrett-Roe, F. Perakis, F. Rao and P. Hamm, *J. Phys. Chem. B*, 2011, **115**, 6976–6984.
63 T. L. C. Jansen, B. M. Auer, M. Yang and J. L. Skinner, *J. Chem. Phys.*, 2010, **132**, 7.
64 H. J. Bakker, Y. L. A. Rezus and R. L. A. Timmer, *J. Phys. Chem. A*, 2008, **112**, 11523.
65 J. B. Asbury, T. Steinel, C. Stromberg, S. A. Corcelli, C. P. Lawrence, J. L. Skinner and M. D. Fayer, *J. Phys. Chem. A*, 2004, **108**, 1107–1119.
66 J. J. Loparo, C. J. Fecko, J. D. Eaves, S. T. Roberts and A. Tokmakoff, *Phys. Rev. B: Condens. Matter*, 2004, **70**, 180201.
67 L. Piatkowski, K. B. Eisenthal and H. J. Bakker, *Phys. Chem. Chem. Phys*, 2009, **11**, 9033–9038.
68 T. Kinugasa, A. Kondo, S. Nishimura, Y. Miyauchi, Y. Nishii, K. Watanabe and H. Takeuchi, *Colloids Surf., A*, 2002, **204**, 193–199.
69 S. Yeremenko, A. Baltuska, F. de Haan, M. S. Pshenichnikov and D. A. Wiersma, *Opt. Lett.*, 2002, **27**, 1171–1173.
70 M. J. Tauber, R. A. Mathies, X. Y. Chen and S. E. Bradforth, *Rev. Sci. Instrum.*, 2003, **74**, 4958–4960.
71 R. G. Gordon, *J. Chem. Phys.*, 1966, **45**, 1643–1648.
72 S. Woutersen and P. Hamm, *J. Phys.: Condens. Matter*, 2002, **14**, R1035–R1062.
73 V. V. Volkov, D. J. Palmer and R. Righini, *Phys. Rev. Lett.*, 2007, **99**, 078302.
74 A. M. Dokter, S. Woutersen and H. J. Bakker, *Phys. Rev. Lett.*, 2005, **94**, 178301.
75 R. E. Miller, *Science*, 1988, **240**, 447–453.
76 T. D. Sechler, E. M. DelSole and J. C. Deák, *J. Colloid Interface Sci.*, 2010, **346**, 391–397.
77 M. Bonn, H. J. Bakker, A. Ghosh, S. Yamamoto, M. Sovago and R. K. Campen, *J. Am. Chem. Soc.*, 2010, **132**, 14971–14978.
78 V. V. Volkov, Y. Takaoka and R. Righini, *J. Phys. Chem. B*, 2009, **113**, 4119–4124.
79 T. I. C. Jansen, D. Cringus and M. S. Pshenichnikov, *J. Phys. Chem. A*, 2009, **113**, 6260–6265.
80 H. Graener, G. Seifert and A. Laubereau, *Chem. Phys.*, 1993, **175**, 193–204.
81 Y. L. A. Rezus and H. J. Bakker, *Phys. Rev. Lett.*, 2007, **99**, 148301.
82 D. E. Moilanen, N. E. Levinger, D. B. Spry and M. D. Fayer, *J. Am. Chem. Soc.*, 2007, **129**, 14311–14318.
83 S. Woutersen, U. Emmerichs, H. K. Nienhuys and H. J. Bakker, *Phys. Rev. Lett.*, 1998, **81**, 1106–1109.